Distributed Navigation Algorithms for Sensor Networks

Chiranjeeb Buragohain, Divyakant Agrawal, Subhash Suri
Dept. of Computer Science, University of California, Santa Barbara, CA 93106, USA
{chiran,agrawal,suri}@cs.ucsb.edu

arXiv:cs/0512060v1 [cs.NI] 14 Dec 2005

***Abstract*— We propose efficient distributed algorithms to aid navigation of a user through a geographic area covered by sensors. The sensors sense the level of danger at their locations and we use this information to find a safe path for the user through the sensor field. Traditional distributed navigation algorithms rely upon flooding the whole network with packets to find an optimal safe path. To reduce the communication expense, we introduce the concept of a skeleton graph which is a sparse subset of the true sensor network communication graph. Using skeleton graphs we show that it is possible to find approximate safe paths with much lower communication cost. We give tight theoretical guarantees on the quality of our approximation and by simulation, show the effectiveness of our algorithms in realistic sensor network situations.**

I. Introduction

Recent advances in computing, communication, and related technologies have resulted in significant interest in sensors and sensor networks. Sensor networks are envisioned as a new link between the physical world and the virtual world as it is modeled by computers, networks, and information. In particular, once the physical world is instrumented with sensors and sensor networks, the information-based model of the physical world changes from a passive one to an active one. Currently, however, sensors are primarily being deployed as information collection points to monitor the physical environment. But as the pace of innovation continues, in not too distant future, it is likely that their scope will grow to allow interaction with as well as control the physical world.

Most of the recent work in sensor networks has been confined to developing technologies for monitoring the physical world. Many applications of sensor networks are indeed in this context: habitat monitoring [1], structural monitoring [2] and counter-sniper systems [3]. Numerous research problems arise in the context of such applications. In particular, a large body of recent research activity in the area of sensor networks has focused on various system level issues such as sensor localization [4], medium access protocols [5], power-efficient routing [6] and distributed query processing [7].

Only recently researchers have begun to explore more sophisticated applications of sensor networks. Instead of viewing a sensor network as a monitoring tool for the physical world, questions are being explored if sensor and sensor networks can transition to become a reactive system. For example, consider a world that has been instrumented with sensors capable of detecting disruptive or dangerous events (e.g., a chemical spill, a traffic accident) and if and when such events occur, the system should be able to aid navigation in the modified state of the physical world. Recently, Li et al. [8] have proposed algorithms to answer exactly this question: guiding the movements of a user through a sensor field in the presence of dangers or obstacles. Their proposed solution finds an optimal safest path, but it is based on the *flooding* model in which every sensor exchanges information with every other sensor. This scheme does not scale well due to a very high communication cost.

In this paper, we propose more scalable solutions for the problem of navigating a user in the presence of disruptions or hazards in a sensor field. Our algorithms make two natural assumptions: (1) the operational environment is assumed to have no large holes in the coverage by sensors, and (2) an *approximately optimal* safe path is acceptable. Based on these two assumptions, we develop distributed navigation algorithms that are very efficient in terms of their communication cost; they find near-optimal paths with significantly smaller communication (and, thus, energy) overhead. The underlying idea behind our scheme is to activate a sparse sub-network within the dense sensor network and use this sparse network to solve the navigation problem. (We envision "rotating" the navigation duties among the sensors so that a small fraction of the network is awake to aid navigation at any point, while other sensors are in the sleep mode.) We explore two different ways to create such sparse embeddings: the first one based on a uniform grid-like mesh, and the other based on an adaptive mesh.

Our main result is that using sparse networks of size $\mathcal{O}(n^{1/2+\epsilon})$, where n is the total number of nodes in the networks, we can determine safe paths whose quality (length, exposure, etc.) is within a small constant factor of the optimal.

II. Preliminaries and Related Work

Let us assume that n sensor *nodes* are placed uniformly in a square area. We choose units of length such that the size of the area is $n^{1/2} \times n^{1/2}$, i.e. on the average every unit area contains one single sensor. Every sensor can communicate with any other sensor which is within radio range r of it. The number of radio neighbors of a single sensor is not large, i.e. $1 < r \ll n^{1/2}$. Thus the sensor nodes form a logical graph with nodes as vertices and communication links between neighbors as edges. Also we assume that each sensor knows its geographic location

The research of the authors were supported by NSF grant CCF-0514738 and Army Reasearch Organization grant DAAD19-03D0004.

through some localization algorithm. The query for safe path is injected into the system at a node which we shall call *source*. The query specifies a destination coordinate. The node closest to the destination coordinate will be called *destination*. The safe path is a path on the communication graph starting at the source and ending at the destination.

A. Metrics for Path Quality

We consider two natural metrics for safe path: path length and exposure. We'll consider two examples to illustrate the relevance of the two metrics in practice. Suppose a dangerous chemical leak has occurred in the region covered by the sensors. We want the safe path from source to destination be such that the maximum concentration of the chemical on the path does not exceed a threshold t. Thus we define the *danger zone* as the region where the chemical concentration exceeds t. The optimal path then is the shortest path between the two points which stays outside the danger zone. We call this the *shortest feasible path* (SFP). In this paper, we shall treat the hop distance in the network and true geometric distance interchangeably. Since our sensors are spread uniformly and they form a dense network, such an assumption will not lead to gross inaccuracies.

The next example is for a point like danger. Let us assume that a sensor detects the presence of an enemy soldier at some point in the battlefield. As we move through the battlefield, the enemy soldier can detect us at a distance by some means, such as sight or sound, but his capacity for detection goes down with distance. Suppose the enemy soldier is at the origin $(0, 0)$ and he can detect us with probability $\phi(x, y)$ if we are at the point (x, y). If we want to move from the source to destination with the least probability of detection, then we need to minimize the following quantity over all possible paths P:

$$\text{Probability of detection} \propto S(P) \equiv \int_P \phi(x, y) d\ell. \quad (1)$$

We call the quantity $S(P)$ as the exposure for the path P and the optimal path as the *minimum exposure path* (MEP). To put it more formally, the presence of enemy at $(0, 0)$, creates a *potential* $\phi(x, y)$ at the point (x, y) and we would like to move along a path where the integrated potential along the path is minimized. The definition of the potential function $\phi(x, y)$ itself is arbitrary, but it should monotonically decrease as we move away from the enemy position. Assuming that the enemy is at the origin, a convenient potential function is

$$\phi(x, y) = \frac{1}{(x^2 + y^2)^{\beta/2}} \equiv \frac{1}{R^\beta}, \quad \beta > 0, \quad (2)$$

where R is the Euclidean distance from the point of danger to the point (x, y). For our purposes in this paper, we shall impose the condition $\beta > 1$. Another desirable property for the potential is the *superposition* property defined as follows. If there are k enemy points denoted by $1, 2, \ldots k$, then the total potential at (x, y) is defined as

$$\phi_{\text{total}}(x, y) = \sum_{i=1}^{k} \phi(x - x_i, y - y_i), \quad (3)$$

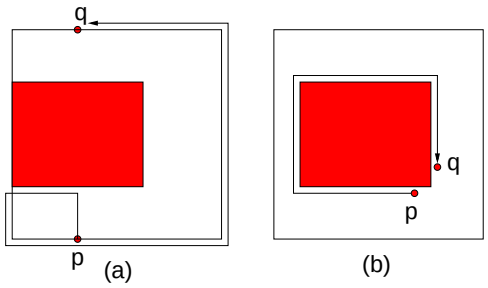

Fig. 1. Bad performance of greedy geographic routing schemes: the source is p and destination is q, while the shaded area represents the danger zone. In (a), the principle of perimeter traversal leads to a traversal of the whole field. In (b), the length of the path found is as large as the perimeter of the danger zone.

where $\phi(x - x_i, y - y_i)$ is the potential at (x, y) due to enemy point i located at (x_i, y_i).

There are some important constraints that one needs to impose on the complexity of the danger zone. In general, if the side-length of the sensor field is $\mathcal{O}(n^{1/2})$, one expects the length of any shortest path be bounded by $\mathcal{O}(n^{1/2})$. But one can easily conjure up pathologically shaped danger zones for which the length of the optimal path can be as long as $\mathcal{O}(n)$. We exclude such exceptional cases by imposing the constraint that the perimeter of the danger zone be "well behaved" in the following sense. Let us consider a curve and a square box of size x which intersects the curve. The well behavedness property restricts the length of the curve inside that box.

Definition 1: A curve is well behaved, if for any square box of side x that intersects the curve, the length of the curve inside the box is less than cx for some constant $c > 1$, and for all x.[1]

This is not a very stringent condition and any polygon of low complexity satisfies it. This property will be key in proving the efficiency of our algorithms. We also demand that the number of distinct dangerous entities be a constant much smaller than $n^{1/2}$.

In summary, the problem which we shall address in this paper is as follows: given an area covered by sensors where one or more danger zones exist, can we efficiently compute approximate shortest paths and minimum exposure paths between any two points?

B. The Skeleton Graph

Navigating a sensor field in the presence of danger zones is a problem which is similar to path planning in the presence of obstacles. There are two obvious ways one can approach this problem: a greedy geographic scheme similar to GPSR routing [9] and exhaustive search. In a geographic scheme, one would greedily move towards the destination and traverse around the danger zones encountered on the way. This scheme has very low communication overhead, but can lead to highly suboptimal paths as shown in Fig. 1. The global exhaustive search algorithm floods the network with packets to carry out

[1]This condition is same as saying that the curve has fractal dimension 1.

a Breadth-First-Search (BFS) on the communication graph. Obviously this algorithm is optimal in terms of path length, but very expensive in terms of communication cost.

Our solution in this direction splits up the problem into two pieces. The first step is to construct a reduced graph with fewer nodes from the full communication graph. We call this smaller graph the *skeleton graph*. The second part is to carry out a search on the skeleton graph to find shortest paths and minimal exposure paths *over the skeleton graph only*. If the skeleton graph is small in size, then even carrying out an exhaustive search over the skeleton graph will not be very expensive in terms of communication. The requirements that we impose on the skeleton graph are as follows: (i) If a safe path exists in the original graph, a safe path exists in the skeleton graph too. (ii) The quality of the path found in the skeleton graph is comparable to the optimal path.

Our main contribution in this work lies in constructing a small sized skeleton graph from the main communication graph. Once the skeleton graph is constructed, the problem of finding the optimal paths on these graphs can be achieved with a set of simple algorithms. These algorithms are *reactive* algorithms rather than *proactive* algorithms. In other words, we do not maintain path information in the system; only when a query is made, path discovery takes place. We briefly discuss these algorithms below. These algorithms are applicable to *any* graph and not special to skeleton graphs in any way.

C. Shortest Path Algorithm

This algorithm is nothing but BFS over the communication graph. The graph is flooded with search packets starting from the source. Every packet contains two fields which specify how many hops it has traveled from the source and the last node visited. When a node receives a search packet, it increments the hop count by 1 and forwards the packet to the other neighbors. Every node maintains a distance variable which counts the minimum number of hops to the source and a parent pointer which points to the node via which the minimum hop search packet was received. If a node receives multiple search packets from the source, only packets with smallest hop counts are forwarded. When BFS terminates, every node knows its distance to the source and its parent pointer points to its parent along the path towards the source.

Note that in a shortest path computation by BFS, the number of packets transmitted by each node is exactly 1. The first search packet that arrives at a node is the packet which has traveled by the least number of hops. The packets which arrive later arrive by traveling larger number of hops and hence are discarded. This leads us to the following proposition which bounds the communication cost of shortest path discovery by BFS search.

Proposition 1: In a network of n nodes, the number of total packet transmissions required for the shortest path algorithm is $\mathcal{O}(n)$.

D. Minimum Exposure Path Algorithm

Algorithm 1 MINIMUM-EXPOSURE

```
1:  while TRUE do
2:    Receive(pkt) from neighbor
3:    pkt.exposure ← pkt.exposure + self.potential
4:    if pkt.exposure < minexposure then
5:      minexposure ← pkt.exposure
6:      parent ← neighbor
7:      schedule pkt for forwarding
8:    else
9:      Drop(pkt)
10:   end if
11:   if there is a scheduled packet then
12:     Transmit(pkt)
13:   end if
14: end while
```

Exposure computation relies upon the computation of potential $\phi(x, y)$ first. We give a simple algorithm for potential calculation below. Assume that the potentials at each point are known. Then minimum exposure path calculation is very similar to the shortest path BFS algorithm. In this case the path length is the total exposure, not total hop count. Search packets are injected into the network by the source and nodes forward these packets to their neighbors. Every search packet carries with itself a variable *exposure* which is just the sum of potentials of the nodes it has passed through. Thus any packet contains within it the total exposure of the path that it has traveled. Just like BFS above, every node maintains a total exposure field (*minexposure*) and a parent pointer. The variable *minexposure* measures the total exposure of the minimum exposure path from the source. Any packet which arrives at a node with total exposure more than the value *minexposure* at that node is not forwarded. Otherwise, the node updates the *minexposure* variable and forwards the packet. The pseudocode is shown in algorithm 1. When the algorithm terminates, every node knows the exposure of the minimum exposure path to the source.

Now we give a simple algorithm to calculate the potential due to a single danger point. Potential due to multiple danger points can be computed using the principle of superposition (eqn. 3). Consider a sensor which detects danger at its location. This sensor floods the network with packets for a BFS much like the shortest path calculation. Thus every node on the network learns its distance from the danger point and hence can now compute the potential according to eqns. 2 and 3.

E. Related Work

Navigation and path planning has a long history as a robotics [10] and computational geometry [11] problem. The challenge for sensor network environment is that path planning must be done in a distributed manner. The problem of route finding in ad-hoc networks is similar to the problem that we address here. Greedy Perimeter Stateless Routing (GPSR) [9] is a greedy routing strategy for ad hoc networks which utilizes geographic information to find its destination. We have

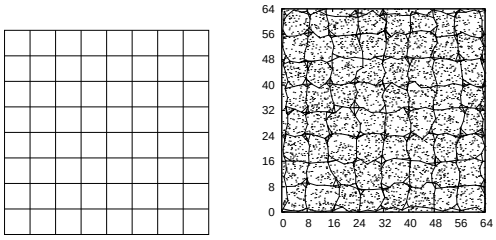

Fig. 2. A street map and the corresponding skeleton graph. There are 4096 nodes with range 3 each. The skeleton graph contains only 450 nodes.

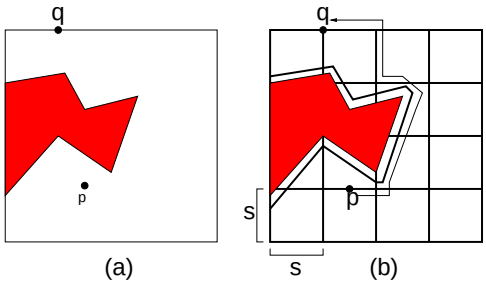

Fig. 3. The street map for uniform skeleton graph. In (a), we show the danger zone as a shaded area and two points p and q between which we seek a shortest path. In (b) we see the street map with grid size s and the streets outlined in bold. The shortest path between p and q is is also shown.

already discussed the unsuitability of geographic schemes for navigation. The alternative protocols like AODV [12] and DSR [13] do not utilize geographic information and instead flood the network with query packets for finding routes. Obviously such a flooding scheme is not efficient for sensor networks.

The concept of minimum exposure path were introduced by Meguerdichian et. al. [14]. Veltri et. al. [15] has given heuristics to distributedly compute minimal and maximal exposure paths in sensor networks. Path planning in the context of sensor networks was addressed by Li et. al. [8] where they consider the problem of finding minimum exposure path. Their approach involves exhaustive search over the whole network to find the minimal exposure path. Recently Liu et.al. [16] have used the concept of searching a sparse subgraph to implement algorithms for resource discovery in sensor networks. This work, which was carried out independently of us, however doesn't address the problem of path finding when parts of the sensor network is blocked due to danger. Some of our work is inspired by the mesh generation problem [11], [17] in computational geometry.

III. Navigation Using Uniform Skeleton Graph

Suppose we have an area A covered with sensors. Then the structure of the skeleton graph can be explained most intuitively in terms of a set of line segments inside this area A. We call these segments *streets* and the collection of all the streets within the area a *street map*. The nodes which are geographically "close" to the streets constitute the skeleton graph. We shall soon define this idea of closeness more rigorously, but meanwhile an example will clarify the concept. Fig. 2 shows a set of streets and the corresponding skeleton graph. All nodes which are not part of the skeleton graph are put to sleep and they do not communicate with other nodes. Thus the skeleton graph is a small set of nodes which geographically span the area A and form within themselves a connected communication graph. The street map is an ideal geometric representation of the skeleton graph and its communication links. The exact algorithm for *embedding* a set of streets in a true network graph will be given in Section III-A. For theoretical purposes in this paper, we shall use the skeleton graph and its abstract street map representation interchangeably.

It is clear that given an arbitrary distribution of sensors and an arbitrary street map, it is not possible to successfully embed the street map in the communication graph. In most realistic settings, the sensors will be deployed in a random fashion, leading to an expected-case uniform coverage of the field. Mathematically, we assume that each sensor's location (x, y) is a pair of independent random variables distributed uniformly. In fact, the only technical requirement of our scheme is that the sensor field not have any large holes in its coverage. Under these conditions and a reasonable radio communication range, it is possible to carry out the embedding. We shall address this issue is a more quantitative fashion in sec. V.

In this section we introduce the uniform skeleton graph which contains two classes of streets: *grid streets* and *perimeter streets*. The grid streets are a square grid of lines separated by distance s from each other. An additional set of streets which follow the perimeter of the danger zone is also included in the street map and they are the perimeter streets. Fig. 3 shows a single danger zone and the street map that results from it.

A. The Uniform Skeleton Graph: Streets and Embeddings

We assume that all nodes know the value of s which is the separation between streets. Then the embedding of the grid streets is achieved as follows. Let us imagine every grid street to be a strip of width w instead of being a line. Since the nodes know their positions, they can independently decide if they are within distance w of any grid street. All nodes which lie on the strip include themselves in the skeleton graph, while the other nodes go to sleep. As long as $wr > 1$, with high probability, the number of nodes lying along the streets is enough to ensure that all the nodes lying along the streets form a connected set. The embedding of the streets can be optimized by an additional step. In general, the strip of width w will contain some redundant nodes which can be put to sleep without losing connectivity. To do this we assign the two nodes at each end of the street to be source and destination. The source carries out a BFS search for the shortest path within this street to the destination. Only the nodes which are on the shortest path from source to destination are included in the skeleton graph.

Note that a protocol like GPSR can be also used construct the grid streets. Let us assume that some node initiates the

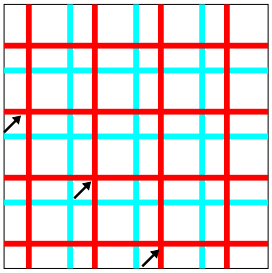

Fig. 4. Load balancing by shifting.

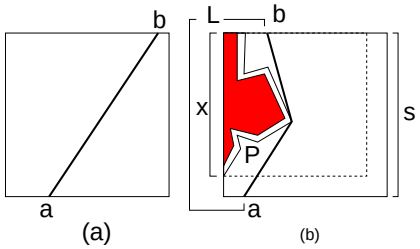

Fig. 5. Shortest path in uniform grid.

street construction protocol. Then using GPSR, we can send out street construction packets along the perpendicular grid lines starting with the initiating node. All nodes which are touched by the construction packets include themselves in the skeleton graph. This method has very low overhead for constructing skeleton graph, but it might produce sub-optimal graphs in the presence of holes.

Next we turn to the embedding of the perimeter streets. To do this, the nodes which are on the danger zone boundary need to detect first that they are on the boundary. This is an easy problem to solve: if a node realizes that it is in the danger zone, but it has at least one neighbor outside the danger zone, then that node declares itself to be at the boundary. The nodes inside the danger zone can go to sleep. The boundary nodes broadcast a "wake-up" message with lifetime of w hops to its neighbors. Any node within w hop of a boundary will be awakened and added to the skeleton graph. These nodes constitute the perimeter streets. Nodes inside the danger zone are always excluded from the skeleton graph.

Once we have constructed the skeleton graph, the shortest path and the minimum exposure paths can be constructed using the algorithms described in sections II-C and II-D. Note that although the skeleton graph requires only a small subset of the nodes to participate in path finding, over time this set of nodes might run out of energy prematurely compared to other nodes which are not included in the skeleton graph. This can be avoided by varying the value of s, the street separation; or by shifting all the streets by a constant amount in the diagonal direction as shown in Fig. 4.

B. Path Discovery for Points not on Streets

So far we have restricted our attention to finding shortest paths between source and destination pairs which are on the streets. What can one do for source and destination pairs which do not lie on any street? There are two solutions. The first solution is for the source to initiate flooding to discover the closest street to it and from then on, follow the streets for route discovery to the destination. If the destination does not lie on any street, then it is enclosed in a square enclosed by four streets. As soon as any packet realizes that it is on the boundary of the square, then the destination can be found by flooding that square. This flooding adds some overhead to path discovery, but this overhead is comparatively low for long paths.

The second solution is to construct the streets on-demand rather than to pre-compute them. As soon as a source needs to discover a route to the destination, it initiates construction of streets centered around itself. We can use GPSR to construct the grid streets as before. The benefit of this approach is that in this case, load balancing is automatic because every path discovery query produces its own set of streets. As mentioned before, this method might be suboptimal if there are significant holes in the communication graph.

C. The Uniform Skeleton Graph: Basic Properties

In this section we focus on the performance characteristics of these algorithms and prove the approximation bounds. We first prove the following theorem which limits the size of the uniform skeleton graph, and hence limits the total communication cost of a search in that graph.

Theorem 1: The communication cost of discovering the shortest path in the uniform skeleton graph is $\mathcal{O}(n^{1/2+\epsilon})$, for any ϵ such that $0 < \epsilon < 1/2$.

Proof: There are two sets of streets: the grid streets and the perimeter streets. Every grid street is of length $n^{1/2}$ and the number of grid streets is $2 \times n^{1/2}/s$. Thus the total length of grid streets is $\mathcal{O}(n/s)$. Since the perimeter of a danger zone is well behaved, the total length of the perimeter as well as the perimeter streets is $\mathcal{O}(n^{1/2})$. The width of the streets w is a constant of order unity, while $1 < s < n^{1/2}$. Clearly, the total street length is dominated by the grid streets. Hence we set $s = n^{1/2-\epsilon}$ and find that the total number of nodes in the skeleton graph is $\mathcal{O}(n^{1/2+\epsilon})$. Applying proposition 1, we immediately see that the communication cost must also be bound by $\mathcal{O}(n^{1/2+\epsilon})$. ■

Note that since $1 < s < n^{1/2}$, ϵ is constrained to lie between 0 and 1/2. The exact choice of ϵ involves a trade-off between skeleton graph size and the quality of path found. A larger value of ϵ, gives better coverage of the area with streets at the expense of involving large number of nodes in the path search.

We now consider the quality of the approximate path length in the uniform skeleton graph. Let us first introduce some notation. Given any two points which are located on streets, there is an optimal path: P_{OPT} and a path along the streets which we call P_{USG}. Their lengths are ℓ_{OPT} and ℓ_{USG} respectively. The following theorem gives the worst case bound on the length of ℓ_{USG}.

Theorem 2: For a path joining any two points located on the streets in uniform skeleton graph,

$$\ell_{\text{USG}}/\ell_{\text{OPT}} \leq 2(1+c),$$

where c is the constant appearing in the definition of well behavedness (Def. 1).

Proof: The optimal path goes through a sequence of grid street squares. We shall decompose the optimal path into segments, each of which is contained completely within its own square. The sides of the square are the streets. If we prove the bound on each square separately, then the total path will also obey the required bound. Consider a segment of the optimal path that goes through a square on the grid and it crosses the square at points a and b (Fig. 5). Since the communication is restricted to move along the streets, there are two paths to get from a to b. There are two cases to take care of while bounding the length of path along the streets.

Fig. 5 (a) exhibits the case when the boundary of the square is free of danger. In that case the shortest path from a to b along the streets is at most twice as long as the optimal path.

Fig. 5 (b) shows the case when one of the sides of the square is blocked by danger. Let's say if the danger was not there, then there would be a path of length L from a to b along the left side of the square. Because of the danger on the edge, the path is forced to traverse the perimeter street P and hence becomes longer. We bound the length of the perimeter street as follows: if the danger zone can be bound within a square of side x, then the length of the perimeter street length is cx by the well behaved property. So total length of the path is at most the sum of the perimeter path length cx and the street length L, i.e. $\ell_{\text{USG}} \leq cx + L$. If $x < L$, $\ell_{\text{OPT}} \geq L/2$ and then

$$\ell_{\text{USG}} \leq cx + L \leq (c+1)L \leq 2(1+c)\ell_{\text{OPT}}.$$

if $x > L$, then the optimal path length $\ell_{\text{OPT}} \geq x$ and

$$\ell_{\text{USG}} \leq cx + L \leq (c+1)x \leq (1+c)\ell_{\text{OPT}}.$$

The case when both sides of the square intersect the perimeter streets can be handled in a similar fashion. ∎

D. The Uniform Skeleton Graph: Exposure

We now consider the minimum exposure path problem. Let us denote the exposure along the true minimum exposure path be S_{OPT}. The minimum exposure using only the skeleton graph is S_{USG}. Before we explore the relation between optimal and approximate exposure, let us prove a useful lemma.

In this lemma, we shall consider a point danger and a path of length L which approaches at its closest to within distance D of the danger point (see Fig. 6). The lemma gives an estimate of the total exposure of this path. Intuitively we can motivate this lemma as follows: for $\beta > 1$, the potential dies fast as one goes away from the danger. So if the closest distance that the path approaches the danger is D, then the major contribution to the exposure comes from a region of size D nearest to the danger. The contribution of the path outside this region contributes to the total exposure only by a constant factor.

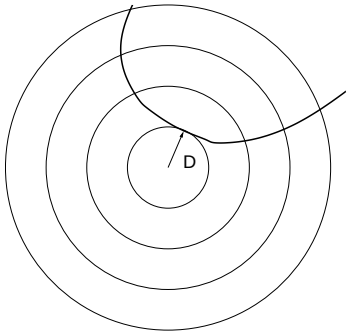

Fig. 6. Exposure along a path.

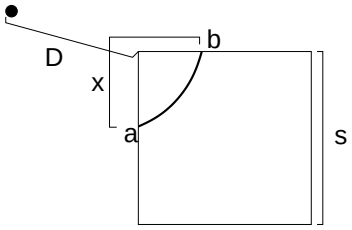

Fig. 7. Exposure along a path in the grid.

Lemma 1: For a well behaved path of length L with minimum approach distance D, and $\beta > 1$, the exposure of the path is given by

$$S = \begin{cases} c_1 \frac{1}{D^{\beta-1}} & L \geq D, \\ c_2 \frac{L}{D^{\beta}} & L < D, \end{cases} \tag{4}$$

where c_1 and c_2 are constants.

Proof: Consider a curve of length $L \geq D$ as shown in Fig. 6. We divide the curve into segments by concentric circles of radius $D, 2D, 3D \ldots$ Since the curve is well behaved, the total length of the curve *inside* a circle of radius kD is bounded by $c_r kD$ for some constant c_r. Consider a segment of the curve contained between circles of radius kD and $(k+1)D$. By the well behaved assumption, the length of this segment is at most $c_a D$ for some constant c_a. So the exposure of this segment is bounded by $\frac{c_a D}{(kD)^\beta}$. The total exposure then is

$$S \leq \sum_{k=1}^{\infty} \frac{c_a D}{(kD)^\beta} = \frac{c_a}{D^{\beta-1}} \sum_{k=1}^{\infty} \frac{1}{k^\beta} \tag{5}$$

The sum on the RHS converges to a constant when $\beta > 1$. The case for $L < D$ is simple. The potential is $\frac{1}{D^\beta}$ and the length of the path is L. The exposure immediately follows from that. ∎

The following theorem bounds the exposure performance of the uniform skeleton graph scheme.

Theorem 3: For a path joining any two points located on the streets,

$$S_{\text{USG}}/S_{\text{OPT}} = \text{const.}$$

Proof: For the sake of brevity, here we give only an outline of the proof of this theorem. As in theorem 2, we shall

decompose the optimal path into segments wholly contained within a single square and prove the bound for a single square. For simplicity we assume that there is a single point of danger as shown in Fig. 7. Let the optimal exposure path cross the square at points a and b. To go from a to b there are two possible paths: a shorter path with exposure S_1 and a longer one with exposure S_2. Their respective lengths are x and $4s-x$ where s is the size of the square. In terms of exposure, the short path has the disadvantage of traversing a region of high potential, while the longer path has the disadvantage of being long.

To compute S_{USG}, we consider the case $x > D$ first as shown in Fig. 7. By lemma 1 the exposures are as follows:

$$S_1 = \mathcal{O}\left(\frac{1}{D^{\beta-1}}\right),\ S_2 = \mathcal{O}\left(\frac{1}{(D+x)^{\beta-1}}\right) \quad (6)$$

$$S_{\text{OPT}} = \mathcal{O}\left(\frac{1}{(D+x)^{\beta-1}}\right). \quad (7)$$

The worst case results when $S_1 = S_2$, which implies that $x = \mathcal{O}(D)$, i.e. S_1, S_2 and S_{OPT} are within constant factor of each other. For $x < D$,

$$S_1 = \mathcal{O}\left(\frac{x}{D^{\beta}}\right),\ S_2 = \mathcal{O}\left(\frac{1}{(D+x)^{\beta-1}}\right) \quad (8)$$

$$S_{\text{OPT}} = \mathcal{O}\left(\frac{x}{(D+x)^{\beta}}\right). \quad (9)$$

The worst case exposure results when $S_1 = S_2$, which implies that $x = \mathcal{O}(D)$, i.e. S_1, S_2 and S_{OPT} are within constant factor of each other.

The case of multiple danger points is a simple generalization. By the principle of superposition, (eqn. 3) the total exposure of a path due to multiple danger points is equal to the sum of exposures due to each danger point taken separately. Thus the proof above remains valid for multiple points of danger as well. ■

IV. Navigation Using Adaptive Skeleton Graph

The uniform skeleton graph is simple and effective, but it is possible to improve upon it. The uniform skeleton graph puts streets with uniform density (all streets have separation s) in every region, without regard for the region's distance from the danger zones. Intuitively, if a user wants to navigate an area with danger zones, it will be useful if near the danger zones, the streets are placed close together, while far away the street layout is much coarser. Readers familiar with computational geometry literature will recognize a similarity of this problem to the problem of adaptive mesh generation [17].

Let us now see how such a non-uniform adaptive street-map can be produced. For this discussion we assume that the danger zone boundary is axis aligned. Our street map will consist of a set of line segments of length $1, 2, 4, \ldots, n^{1/2}$ which are also axis aligned. The logical representation of the street map can be best done in terms of a quadtree. This process is very similar to quadtree mesh generation. The whole $n^{1/2} \times n^{1/2}$ square area corresponds to the root node in the quadtree. We recursively divide the area into quadtree cells until there is no quadtree cell whose boundary is intersected by danger zone boundary. The process is illustrated in Fig. 8. In the next section we show that this adaptive construction is not only more efficient in terms of number of nodes involved, but also has better guarantees on total path length compared to the uniform skeleton graph.

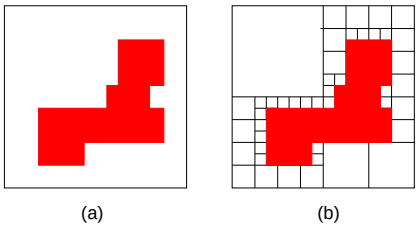

Fig. 8. Street map for a danger zone using a four level quadtree. (a) shows the danger zone as the shaded area. In (b) we see the quadtree division so that boundary of the danger zone is completely aligned with the quadtree.

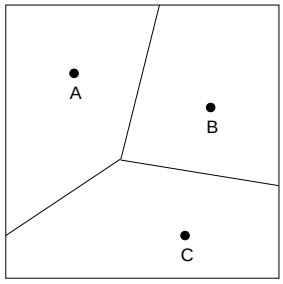

Fig. 9. Voronoi streets for three points of danger.

Note that, having more detailed street map near the danger zones is efficient for computing shortest paths, but it is not efficient for computing minimum exposure paths. Consider for example the three points of danger inside the coverage area as shown in Fig. 9. Since the minimum exposure path should stay as far away from the danger points as possible, intuitively the best one can do is to move along the Voronoi edges [11] for the three points. Thus for computing minimum exposure paths, we would want to compute Voronoi edges for the danger points and embed them using the quadtree.

A. The Adaptive Skeleton Graph: Streets and Embeddings

The quadtree street map can be created in a distributed fashion, but it requires a little coordination among sensor nodes. At this point we shall be a little loose with terminology and use the word node to denote a true physical sensor as well as a node on the abstract quadtree representation of the street map. No confusion should arise though, because the meaning will be clear from the context.

A quadtree node of level k in physical terms consists of a square of side length 2^k. The sensor nodes which lie within distance $w/2$ of the boundary of the square correspond to a *cluster*. We shall assign a single node in the cluster to be a *cluster leader* for that cluster. The cluster leader can be elected using any suitable leader election algorithm. Note that a single segment of an edge in the quadtree can be part of several

squares of different sizes. Thus a single sensor can belong to multiple clusters. The communication primitive required by an ordinary node is very simple. It needs to be able to send a message to its cluster leader and forward any message to its neighbor. The cluster leader has more responsibility. It can communicate with its cluster by sending a message which traverses the boundary of the square. A cluster leader also needs to know the leaders of its parent cluster and children clusters

The quadtree is built recursively. At the beginning the quadtree consists of all the leaf squares and hence the skeleton graph consists of all nodes. If a cluster leader of a leaf square determines that none of its nodes are within the danger zone, then it sends a message informing its parent cluster leader of this fact. If a parent cluster determines that all its children are danger free, then it can instruct its children to go to sleep. This process repeats recursively up the quadtree all the way to the root. The skeleton graph then consists of all the clusters which are still awake.

The embedding of Voronoi edges can be done in a very similar manner. To compute nodes which are on the Voronoi edge, we adopt the following algorithm. Recall that every sensor located at a danger point carries out a potential computation (Section II-D) which is nothing but a BFS distance computation. A node which finds that it is equidistant from any two danger points declares itself to be on a Voronoi edge. Once the Voronoi edges are computed, embedding them using a quadtree can be done as outlined above.

B. The Adaptive Skeleton Graph: Properties

The following theorem shows that the adaptive skeleton graph is highly efficient in terms of total number of nodes in the graph.

Theorem 4: The communication cost of discovering the shortest path in the adaptive skeleton graph is $\mathcal{O}(n^{1/2}\log n)$.

Proof: For simplicity we shall assume that there is only one danger zone with perimeter length p. By the assumption that the perimeter is well behaved, $p = \mathcal{O}(n^{1/2})$. Let us number the quadtree levels as $0, 1, 2, \ldots$ with level 0 as the leaf level. Thus the quadtree level of k corresponds to a square of side 2^k. Since the perimeter length is p, the perimeter is adjacent to p squares of level 0. By the same logic, the perimeter crosses $p/2$ nodes of level 2, $p/4$ nodes of level 2 and so on. In general the perimeter crosses $p/2^k$ nodes of level k (size 2^k), and hence requires $p/2^k$ nodes in its representation. These $p/2^k$ nodes contribute a total of $\mathcal{O}(p/2^k \times 2^k) = \mathcal{O}(p)$ length of streets to the street map. Since there are a total of $\log(n)$ levels in the quadtree, the total length of streets in the quadtree is $\mathcal{O}(p \log n) = \mathcal{O}(n^{1/2}\log n)$. The length of streets in the quadtree immediately gives us the upper bound on the number of nodes in the adaptive skeleton graph and by proposition 1, the upper bound on the communication cost of the shortest path computation. ■

Now we turn to the issue of path lengths and exposure in the adaptive skeleton graph. Here we can mostly take over the discussion that we have gone over in Section III and simplify the proofs. The following theorem shows that the adaptive skeleton graph is very efficient in terms of shortest path. Let the length for the shortest path in the quadtree grid be ℓ_{ASG}.

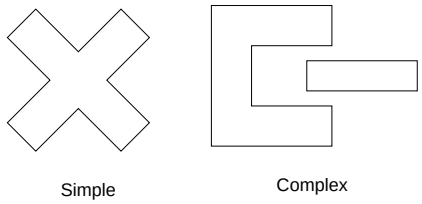

Fig. 10. Simple and complex danger zone shapes used to test shortest path algorithms.

Theorem 5: For a path joining any two points located on the streets in the adaptive skeleton graph,

$$\ell_{\text{ASG}}/\ell_{\text{OPT}} \leq 2.$$

Proof: The optimal path passes through a set of quadtree squares. Unlike the uniform skeleton graph, in the adaptive skeleton graph none of the squares are intersected by the danger zone boundary. Now consider a segment of the optimal path going through a single square as shown in Fig. 5 (a). It is clear that a path which sticks to the sides of the square is at most twice long as the optimal path. ■

The performance bound for the minimum exposure path for the adaptive skeleton graph is identical to the uniform skeleton graph. Note that in theorem 3, the size of the square itself did not appear anywhere. Hence that proof can serve without any modification for the following theorem:

Theorem 6: For a path joining any two points located on the streets in adaptive skeleton graph,

$$\frac{S_{\text{ASG}}}{S_{\text{OPT}}} = \text{const},$$

where S_{ASG} is the exposure for the adaptive skeleton graph.

V. Experimental Results

We simulated our algorithms on simulated communication graph topologies. The simulation parameters are as follows. We place n sensor nodes in a $\sqrt{n} \times \sqrt{n}$ area. The node coordinates are random variables uniformly distributed within this area. The experiments were done with $n = 1024, 4096$ and 16384 nodes. Note that the average separation between nodes in our experiments is 1. So the radio range decides the number of communication neighbors of each node and is an indirect measure of node deployment density. Experimentally we find that unless radio range is larger than 1.5, the resulting graph is almost always disconnected. Even when the communication graph is connected, because of random fluctuations in node density there are always large voids in the communication graph. These voids are known to cause significant problems for geographic routing protocols [9]. For our experiments we assume that the radio range is 3 and in this range the occurrence of large voids is rare. Note that this is not a very dense deployment of nodes. For MICAz motes manufactured

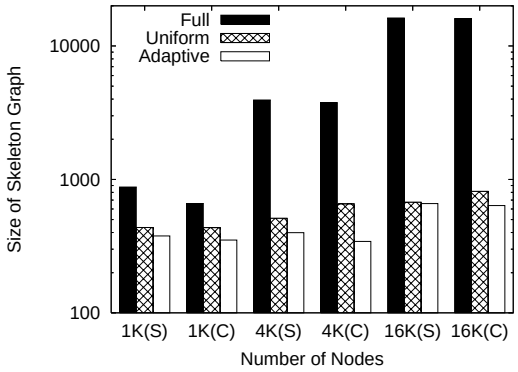

Fig. 11. Number of nodes in skeleton graph for different sized networks. The label 1K(S) means 1024 nodes with simple danger zone, 16K(C) means 16384 nodes with complex danger zone etc. The exponent $\epsilon = 0.05$. Note that the vertical scale is logarithmic.

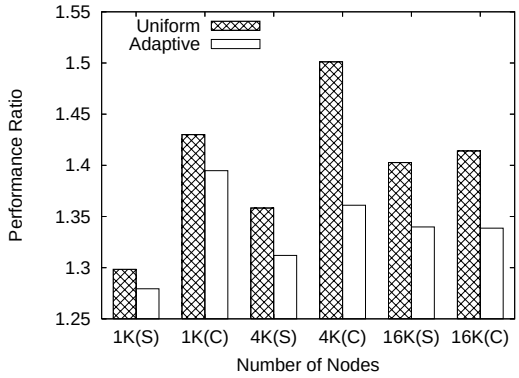

Fig. 12. Path length performance ratio of the uniform and adaptive skeleton graphs for different network sizes. The label 1K(S) means 1024 nodes with simple danger zone, 16K(C) means 16384 nodes with complex danger zone etc. The exponent $\epsilon = 0.05$.

by the Crossbow Corp. [18] which have radio range of 300ft, this works out to a deployment where average node separation is 100ft.

The shortest path algorithms were implemented for two different types of danger zones which we label *simple* and *complex*. Their shapes are shown in Fig. 10. The skeleton graph is a complex experimental system where one can measure many relevant quantities such as the effect of varying size and shapes of danger zones, effect of street separation s on path lengths and others. In the interest of space, we only report the results of a limited set of experiments which evaluate the size of skeleton graphs and their performance in finding shortest paths and minimum exposure paths.

A. Skeleton Graph Size

In Fig. 11, we exhibit the size of the skeleton graph for different shapes of danger zones and different number of sensors. As we can see, the size of the skeleton graphs are much much smaller than the full graph and this difference is more pronounced for larger network sizes. For a network of 1024 sensors and a simple danger zone, the size of the adaptive skeleton graph is only 377, i.e. 37% of the original graph. When we increase network size to 16384, there are 659 nodes are in the adaptive skeleton graph —-which is only 4% of the full graph. The uniform skeleton graph is slightly larger than the adaptive graph, but this difference is not highly significant.

B. Shortest Path

To evaluate the quality of the shortest path found in the skeleton graph we generated a set of 200 random point pairs lying within the sensor coverage area. Let us assume that the lengths of the optimal path and approximate skeleton graph paths are $\ell_{\rm OPT}$ and $\ell_{\rm SG}$ respectively. Then the efficiency of the algorithms is defined by the Path Length Performance Ratio $\equiv \ell_{\rm SG}/\ell_{\rm OPT}$. Closer the performance ratio to 1, better the algorithm. In Fig. 12 we plot the average performance ratio for both uniform and adaptive skeleton graphs. The optimal path was found by carrying out BFS over the full graph. We see that for a large range of network sizes and a combination of simple as well as complex danger zones, the approximate path lengths are no worse than 50% of the optimal. The adaptive skeleton graph performs better as expected.

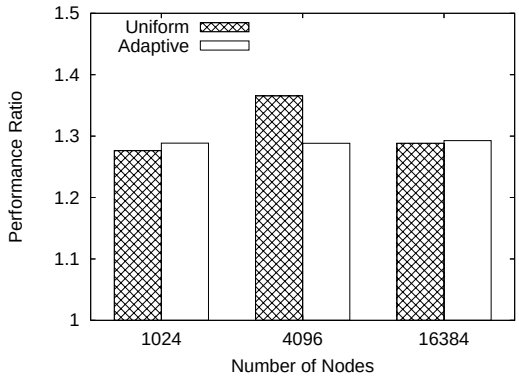

Fig. 13. Exposure performance ratio of the uniform and adaptive skeleton graphs for different network sizes. The exponent $\epsilon = 0.2$.

C. Minimum Exposure Path

For minimum exposure path we generated 20 different scenarios, each of which consists of three points of danger randomly placed inside the coverage area. For each set of three points we computed 10 minimum exposure paths using the skeleton graph. The exponent ϵ was chosen such that the size of the uniform skeleton graph was roughly equal to the size of the adaptive graph. The optimal exposure was calculated by BFS over the full graph as before. If the exposures for optimal and approximate paths are $S_{\rm OPT}$ and $S_{\rm SG}$, we define the performance ratio as before to be Exposure Performance Ratio $\equiv S_{\rm SG}/S_{\rm OPT}$. The average performance ratio is plotted in Fig. 13. As we can see both the uniform and adaptive skeleton graphs perform equally well with neither holding a decisive advantage.

VI. Discussion

We have shown that the problem of finding shortest path and minimum exposure path on a sensor network can be solved approximately with low communication cost using skeleton graphs. Our experiments confirm that both the uniform and adaptive skeleton graphs provide close to optimal paths with very low communication overhead. Although, in the asymptotic limit of large networks, adaptive skeleton graph is more scalable, this is not a real issue for realistically sized networks. Moreover as we have noted in the end of sec. III-A, there exists simple load balancing schemes for uniform skeleton graph. Thus from the perspective of a practical implementation, the uniform skeleton graph is superior to the adaptive graph in terms of its simplicity and load distribution.

References

[1] R. Szewczyk, A. Mainwaring, J. Polastre, and D. Culler, "An analysis of a large scale habitat monitoring application," in *Proc. of SenSys '04*, 2004.

[2] N. Xu, S. Rangwala, K. Chintalapudi, D. Ganesan, A. Broad, R. Govindan, and D. Estrin, "A wireless sensor network for structural monitoring," in *Proc. of SenSys '04*, 2004.

[3] G. Simon, A. Ledeczi, and M. Maroti, "Sensor network-based countersniper system," in *Proc. of SenSys '04*, 2004.

[4] D. Moore, J. Leonard, D. Rus, and S. Teller, "Robust distributed network localization with noisy range measurements," in *Proc. of SenSys '04*, 2004.

[5] J. Polastre, J. Hill, and D. Culler, "Versatile low power media access for wireless sensor networks," in *Proc. of SenSys 2004*.

[6] J. Aslam, Q. Li, and D. Rus, "Three power-aware routing algorithms for sensor networks," *Wireless Communications and Mobile Computing*, vol. 3, no. 2, pp. 187–208, March 2003.

[7] S. Madden, M. Franklin, J. Hellerstein, and W. Hong, "Tag: a tiny aggregation service for ad-hoc sensor networks," in *Proc. of OSDI '02*, 2002.

[8] Q. Li, M. DeRosa, and D. Rus, "Distributed algorithms for guiding navigation across a sensor network," in *Proc. of IPSN '03.*, 2003.

[9] B. Karp and H. T. Kung, "GPSR: greedy perimeter stateless routing for wireless networks," in *Proc. of MOBICOM 2000*.

[10] J.-C. Latombe, *Robot Motion Planning*. Kluwer, 1992.

[11] M. de Berg, O. Schwarzkopf, M. van Kreveld, and M. Overmars, *Computational Geometry: Algorithms and Applications, Second Edition*. Springer-Verlag, 2000.

[12] C. E. Perkins, E. M. Belding-Royer, and S. Das, *Ad Hoc On Demand Distance Vector (AODV) Routing.* IETF RFC 3561.

[13] D. B. Johnson, D. A. Maltz, and Y.-C. Hu, *The Dynamic Source Routing Protocol for Mobile Ad Hoc Networks (DSR).* IETF Internet draft.

[14] S. Meguerdichian, F. Koushanfar, G. Qu, and M. Potkonjak, "Exposure in wireless ad-hoc sensor networks," in *Proc. of MOBICOM 2001*, 2001.

[15] G. Veltri, Q. Huang, G. Qu, and M. Potkonjak, "Minimal and maximal exposure path algorithms for wireless embedded sensor networks," in *Proc. of SenSys 2003*, 2003.

[16] X. Liu, Q. Huang, and Y. Zhang, "Combs, needles, haystacks: Balancing push and pull for discovery in large-scale sensor networks," in *Proc. of SenSys '04*, 2004.

[17] M. Bern and D. Eppstein, "Mesh generation and optimal triangulation," pp. 23–90., 1992.

[18] *MICAz ZigBee Series (MPR2400) datasheet.* Crossbow Technology, `http://www.xbow.com`, 2004.